

**THE FUNDAMENTAL PLANE OF FIELD EARLY-TYPE GALAXIES  
AT INTERMEDIATE REDSHIFT**

Tommaso Treu<sup>1,2</sup>, Massimo Stiavelli<sup>2</sup>, Stefano Casertano<sup>2,3</sup>, Palle Møller<sup>4</sup>, Giuseppe Bertin<sup>1</sup>

<sup>1</sup> Scuola Normale Superiore, P.za dei Cavalieri 7, I56126, Pisa, Italy

<sup>2</sup> Space Telescope Science Institute, 3700 San Martin Dr., Baltimore, MD 21218, USA

<sup>3</sup> On assignment from the Space Science Division of the European Space Agency

<sup>4</sup> ESO, Karl-Schwarzschild Str. 3, D85748, Garching bei München, Germany

ABSTRACT

We present preliminary results on the evolution of the stellar populations of field early-type galaxies (E/S0) from  $z = 0.4$  to  $z = 0$ . The diagnostic tool used in this study is the Fundamental Plane (FP), a tight empirical correlation between their central velocity dispersion ( $\sigma$ ), effective radius ( $R_e$ ), and effective surface brightness ( $SB_e$ ), which is observed to hold in the local Universe. Using HST-WFPC2 archive images and spectra obtained at the ESO-3.6m telescope we measured the FP parameters for a sample of  $\sim 30$  field E/S0s at  $z = 0.2 - 0.4$ . Remarkably, field E/S0s at intermediate redshift also define a tight FP, with scatter unchanged with respect to that of local samples. The intermediate redshift FP is offset from the local one, in the sense that, for given  $R_e$  and  $\sigma$ , galaxies are brighter at  $z = 0.4$  than at  $z = 0$ . The implication of the offset of the FP in terms of passive evolution of the stellar population depends on its star formation history. In a single burst scenario, the stellar populations of field E/S0s were formed at  $z = 0.8 - 1.6$  ( $\Omega = 0.3$ ;  $\Omega_\Lambda = 0.7$ ;  $H_0 = 50$  km s<sup>-1</sup>Mpc<sup>-1</sup>). Alternatively, the bulk of stars (90% in mass) can be formed at high redshift ( $z \sim 3$ ), and the rest in a secondary burst occurred more recently ( $z \sim 0.5 - 0.8$ ).

Keywords: galaxies: elliptical and lenticular, cD—galaxies: evolution—galaxies: photometry—galaxies: kinematics and dynamics—galaxies: fundamental parameters—galaxies: formation

1. Introduction

Understanding the formation and evolution of field early-type galaxies is a cornerstone for the entire picture of galaxy formation. In fact, one of the predictions of hierarchical clustering models is that early-type galaxies and their stellar populations form much later in the field than in the core of rich clusters. This is due to the fact that for a random Gaussian initial density field the collapse of density peaks occurs earlier in the proximity of the large scale overdensities that are bound to be the location of present day clusters (Kauffmann, 1996). A number of stud-

ies have shown that the stellar populations of early-type galaxies in the core of rich clusters are homogeneously old (Bower, Lucey & Ellis, 1992; Ellis et al. 1997; Stanford et al. 1998; van Dokkum et al. 1998; Brown et al. 2000). The few results collected so far in the field environment indicate that the star formation history is more complex than what is suggested by the canonical scenario of passive evolution of an old stellar population (see e. g. Schade et al. 1999; Treu & Stiavelli, 1999, and references therein). We report here on a project that we have just completed, aimed at gathering new information on the star formation history of field early-type galaxies by studying the evolution of the Fundamental Plane with redshift as a diagnostic of stellar populations.

The Fundamental Plane (hereafter FP; Djorgovski & Davis 1987; Dressler et al. 1987) of early-type galaxies is defined as

$$\log R_e = \alpha \log \sigma + \beta SB_e + \gamma, \quad (1)$$

where  $R_e$  is the effective radius in kpc,  $\sigma$  is the central velocity dispersion in km s<sup>-1</sup>,  $SB_e$  is the average surface brightness within the effective radius in mag arcsec<sup>-2</sup>. In the following we refer, when needed, to  $H_0 = h_{50} 50$  km s<sup>-1</sup>Mpc<sup>-1</sup> and to a  $\Lambda$  cosmology ( $\Omega = 0.3$ ;  $\Omega_\Lambda = 0.7$ ).

A simple physical interpretation of the FP (Faber et al. 1987) can be given by defining an effective mass,

$$M \equiv \frac{\sigma^2 R_e}{G}, \quad (2)$$

suggested by the Virial Theorem, by defining the luminosity in the usual way

$$-2.5 \log L \equiv SB_e - 5 \log R_e - 2.5 \log 2\pi, \quad (3)$$

and by considering an effective mass-luminosity relation of the form

$$L \propto M^\eta. \quad (4)$$

These assumptions lead directly to the FP relation given above, provided

$$\alpha - 10\beta + 2 = 0, \quad (5)$$

(van Albada et al. 1995), with  $\eta = 0.2\alpha/\beta$ . In this framework, variations of the slopes  $\alpha$ ,  $\beta$  and the intercept  $\gamma$  (typical values at  $z \approx 0$  are 1.25, 0.32, -8.895,

in Johnson B band, so that  $\eta \approx 0.8$ ; see Bender et al. 1998) as a function of redshift are easily interpreted as general trends in the luminosity evolution of the galactic stellar population. In particular, if we assume fixed slopes and define for an individual galaxy (labeled by the superscript  $i$ )

$$\gamma^i \equiv \log R_e^i - \alpha \log \sigma^i - \beta \text{SB}_e^i, \quad (6)$$

the offset with respect to the prediction of the FP ( $\Delta\gamma^i \equiv \gamma^i - \gamma$ ) is related to the offset of the  $M/L$  by

$$\Delta \log \left( \frac{M}{L} \right)^i = -\frac{\Delta\gamma^i}{2.5\beta}. \quad (7)$$

Similarly, the scatter (rms) of the FP can be related to the scatter in the  $M/L$  at a given  $M$ :

$$\text{rms} \left( \log \frac{M}{L} \right) = \frac{\text{rms}(\gamma)}{2.5\beta}. \quad (8)$$

Therefore the very existence of the FP constrains the similarity of the stellar populations of early-type galaxies, and it is interesting to explore how far in the past this similarity extends.

Recently, using the Hubble Space Telescope (HST) for photometry and ground-based spectroscopy from large telescopes, the FP parameters of cluster E/S0s have been measured out to  $z \approx 0.8$  (Pahre et al. 1995; van Dokkum & Franx 1996, hereafter DF96; Kelson et al. 1997, hereafter K97; Bender et al. 1998; van Dokkum et al. 1998; Kelson et al. 2000). The data show that the FP is well-defined up to look-back times of  $\sim 7.5$  Gyrs, indicating that the origin of the relation is hidden at still higher redshift. The evolution of the intercept is consistent with what is predicted by the passive evolution of an old stellar population in a  $\Lambda$  cosmology ( $z_f \sim 2$ ; van Dokkum et al. 1998).

In a pilot study of a sample of six early-type galaxies at intermediate redshift (Treu et al. 1999; hereafter T99) we found that the FP is also well defined in the field environment out to  $z \approx 0.3$ . We have now collected a larger sample of data. In this paper we give a preliminary report of this study (the complete data-set will be presented in Treu et al. 2000a, the complete analysis in Treu et al. 2000b). In Section 2 we summarize the observational results and describe the location and scatter of the intermediate redshift field FP. In Section 3 we briefly discuss the results in terms of passive evolution of the stellar populations.

## 2. The field FP at intermediate redshift

A sample of early-type galaxies was selected from the Wide Field and Planetary Camera 2 Medium Deep Survey (Griffiths et al. 1994) archival images on the basis of morphology, color, and magnitude (see T00a for a discussion of the sample selection and data analysis). Follow-up spectroscopy was obtained at the ESO-3.6m telescope, yielding accurate velocity dispersions for 22 galaxies in the sample ( $z \approx 0.2 - 0.4$ ).

In Figure 1, panels (a), (b), and (c), we plot the location in the FP space of the intermediate redshift

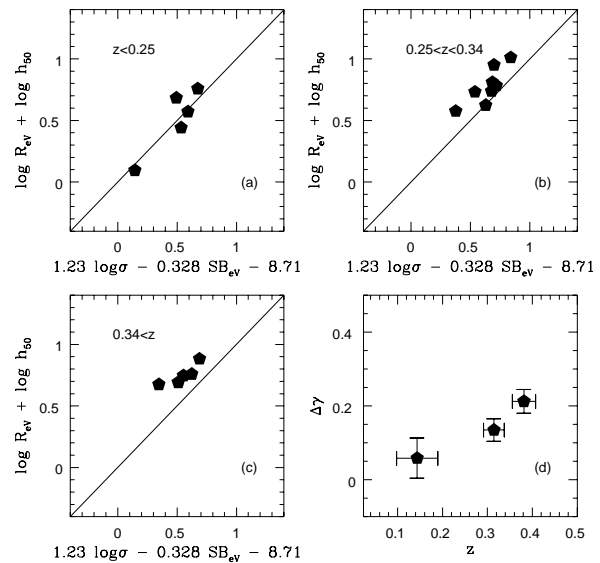


Figure 1. Fundamental Plane in V band (rest frame) at intermediate redshift. In panels (a), (b), and (c) we plot the intermediate redshift galaxies (pentagons) binned in redshift. The solid line represents the FP of Coma, as measured by Lucey et al. (1991). In panel (d) the average offset of the intercept (with fixed slopes taken from Lucey et al. 1991) is plotted as a function of redshift. The error bars in panel (d) are the standard deviation of the mean. The errors in panels (a), (b), and (c) are not shown in this edge-on projection of the FP, since errors on the photometric parameters are correlated (see T00a,b).

data points binned in redshift. The data are in rest frame V band. The solid line represents the FP of the Coma Cluster (Lucey et al. 1991). In panel (d) we show the evolution of the intercept with redshift, with respect to the Coma relation. Qualitatively, two main facts are evident:

1. At any given redshift between 0 and  $\approx 0.4$  the FP of *field* early type galaxies is well defined. The scatter is small. No trend of increasing scatter with redshift is noticeable within the accuracy allowed by the small number statistics available (see Figure 2).
2. The intermediate redshift data points at given  $\text{SB}_e$  and  $\sigma$  have larger effective radii than the value predicted by the local relation (solid line), and hence are more luminous. The average offset increases with redshift as shown in panel (d).

We can quantify these statements by describing the evolution of the intercept with a simple linear relation  $\Delta\gamma = \tau z$  (Figure 2). A least  $\chi^2$  fit yields  $\tau = 0.54 \pm 0.02$ . Taking into account selection effects (see T00b) the 68 % confidence interval is  $0.44 < \tau < 0.56$ . This description allows us to estimate the scatter of the FP in any redshift bin. In fact, there are three contributions to the scatter: the measurement scatter, the intrinsic scatter, and the evolutionary scatter. The latter is simply the combined effect of the thickness of the redshift bins and

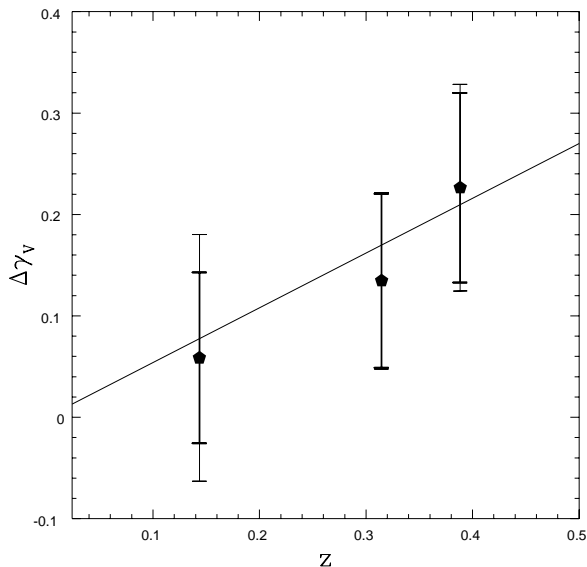


Figure 2. Evolution of the intercept of the FP and its scatter with redshift. The solid line is a least  $\chi^2$  linear fit to the data. The thin error bars are the measured scatter, the thick error bars are the scatter corrected for its evolutionary component (see text).

the evolution of the intercept. We can correct the measured scatter for this projection effect by “evolving” linearly the galaxies to the average redshift of the bin. The corrected scatter obtained in this way is remarkably small and constant (0.08-0.09 in  $\gamma$ , including measurement scatter  $\approx 0.05$ -0.06). Given the limited number of data points available per redshift bin the error on the scatter is quite large ( $\sim 30\%$  for a Gaussian distribution, neglecting systematics); still a substantial increase in the scatter can be ruled out. Larger samples are needed in order to measure the scatter as a function of redshift accurately.

### 3. Evolution of the stellar populations

In this section we compare the observed results on the FP at intermediate redshift with the prediction of stellar population evolution models (Bruzual & Charlot, 1993; GISSEL96 version, hereafter BC96). To this aim we assume that the only evolving factor is the stellar population, that the slopes of the FP do not change with redshift, and that the stellar mass  $M_*$  is proportional to  $M$ . Under these assumptions

$$\Delta \log \frac{M_*}{L} = -\frac{\Delta \gamma}{2.5\beta}, \quad (9)$$

where  $\Delta$  indicates the difference of the quantity with respect to the value found in Coma. In Figure 3 the evolution of the FP is compared with the prediction of single burst stellar population models formed at different formation redshifts ( $z_f$ ). A quantitative comparison is made in Figure 4 where the probability density of  $z_f$  given the observations is shown. The probability density is obtained with a Bayesian-Montecarlo method described in T00b and takes into account the selection effects. The probability peaks

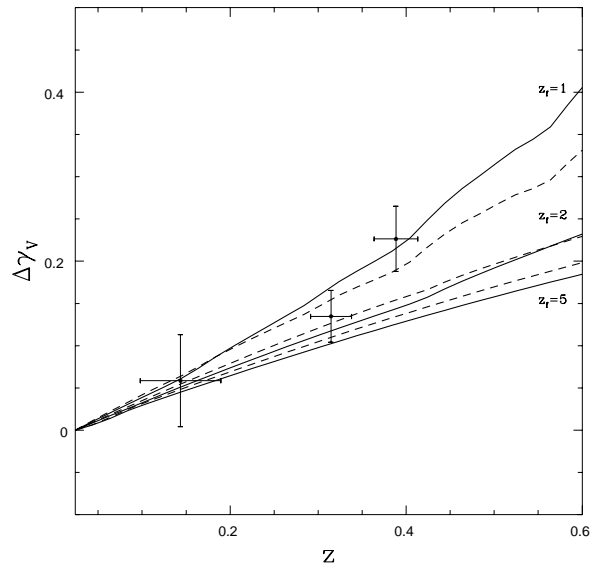


Figure 3. Single burst passive evolution models. The evolution of the intercept of the FP is compared with the prediction of single burst passive evolution models computed from BC96 synthetic spectra. The solid lines represent models with Salpeter IMF (Salpeter, 1955), the dashed lines represent models with Scalo IMF (Scalo, 1986). All models have solar metallicity. Three redshifts of formation are assumed,  $z_f=1, 2$ , and 5, from top to bottom.

at  $z_f \sim 1$  extending from  $z_f = 0.8$  to  $z_f = 1.6$ , corresponding to present ages of 7-10 Gyrs.

The single burst stellar population model is very useful as a benchmark to quantify and compare different results. However, it is clearly just a simplified picture of the star formation history of early-type galaxies. A small amount ( $< 10\%$ ) of the total mass of moderately young stars (one Gyr or so) can alter in a significant way the integrated colors and the  $M_*/L$  of an old stellar population. In this scenario, after a few Gyrs, the integrated colors and the  $M_*/L$  become totally indistinguishable from the ones of an old single burst stellar population. A wealth of observational evidence suggests that minor episodes of star formation can occur from intermediate redshifts to the present (e. g. Schade et al. 1999; Bernardi et al. 1998), and it is worth addressing this issue for our sample of field early-type galaxies. With an analysis similar to that for the single component case we obtained (T00b) the probability density for the redshift of formation of two stellar components: an older one formed at  $z_{f1}$  and a younger one, 10 times smaller in mass, formed at  $z_{f2}$ . The contour levels of the probability density corresponding to 68% and 95% probability are shown in Figure 5. Not surprisingly, it is sufficient to have a small mass of stars formed at  $z < 0.6 - 0.8$  to make it possible for the rest of the stellar mass to be formed at the very beginning of the Universe ( $z_{f1} \sim 3-4$ , i. e. 12-13 Gyrs ago). This scenario is also consistent with the small scatter observed for the FP at low and intermediate redshift, in the sense that the scatter in the FP due to the composite ages of stellar populations is always smaller than the observed one.

## Acknowledgments

This research has been partially funded by the Ministero dell'Università e della Ricerca Scientifica e Tecnologica, by the Space Telescope Science Institute (STScI) Director Discretionary Fund grants 82216 and 82228, by the Agenzia Spaziale Italiana. It is based on observations collected at the European Southern Observatory, La Silla, Chile (Proposals 62.O-0592, 63.O-0468, 64.O-0281) and with the NASA/ESA HST, obtained at the STScI, which is operated by AURA, under NASA contract NAS5-26555.

## REFERENCES

- Bender R., Burstein D., Faber S. M., 1992, ApJ, 399, 462
- Bender R., Saglia R. P., Ziegler B., Belloni P., Greggio L., Hopp U., Bruzual G., 1998, ApJ, 493, 529
- Bernardi M. et al. 1998, ApJ, 508, L43
- Bower R. G., Lucey J. R., Ellis R. S., 1992, MNRAS, 254, 601
- Brown T. et al. 2000, ApJ, 529, 89
- Bruzual A. G., Charlot S., 1993, ApJ, 405, 538
- Djorgovski S., Davis M., 1987, ApJ, 313, 59
- Dressler A., Lynden-Bell D., Burstein D., Davies R. L., Faber S. M., Terlevich R. J., Wegner G., 1987, ApJ, 313, 42
- Griffiths E. et al. 1994, ApJ, 435, L19
- Ellis R., et al. 1997, ApJ, 483, 582
- Kauffmann G., 1996, MNRAS, 281, 487
- Kelson D. D., van Dokkum P. G., Franx M., Illingworth G. D., Fabricant D., 1997, ApJ, 478, L13
- Kelson D. D., van Dokkum P. G., Franx M., Illingworth G. D., 2000, 531, 184
- Lucey J. R., Guzmán R., Carter D., Terlevich R.J., 1991, MNRAS, 253, 584
- Pahre M. A., Djorgovski S.G., De Carvalho R.R., 1995, AAS, 187, #110.08
- Salpeter E., 1955, ApJ, 121, 161
- Scalo J., 1986, Fund. Cosmic Phys., 11, 1
- Schade D. et al. 1999, ApJ, 525, 31
- Stanford S. A., Eisenhardt P. R., Dickinson M. E., 1998, ApJ, 492, 461
- Treu T. & Stiavelli M., 1999, ApJ, 524, L27
- Treu T., Stiavelli M., Casertano S., Møller P., Bertin G., 1999, MNRAS, 308, 1307 (T99)
- Treu T., Stiavelli M., Casertano S., Møller P., Bertin G., 2000, in preparation (T00a)
- Treu T., Stiavelli M., Casertano S., Møller P., Bertin G., 2000, in preparation (T00b)
- van Albada T. S., Bertin G., Stiavelli M., 1995, MNRAS, 276, 1255
- van Dokkum P., Franx M., 1996, MNRAS, 281, 985
- van Dokkum P., Franx M., Kelson D., Illingworth, G. D., 1998, ApJ, 504, L17

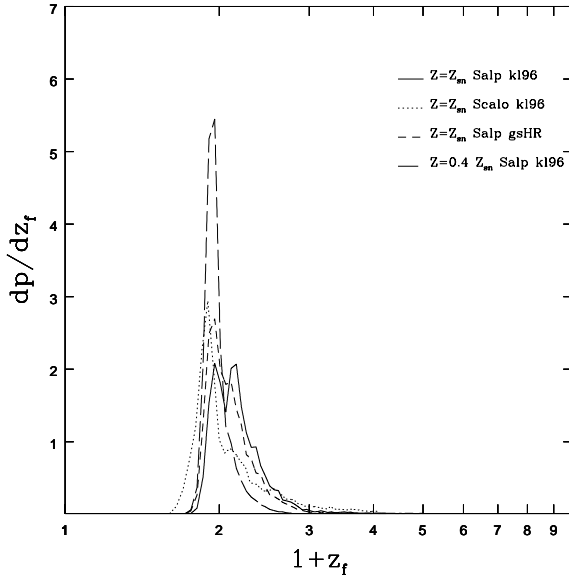


Figure 4. Single burst stellar population models. The probability density of the redshift of formation for various realizations of the models. Spectral synthesis models from BC96 are used with Salpeter and Scalo IMF, solar and 0.4 solar metallicity, atmosphere from Kurucz or Gunn & Striker (see Bruzual & Charlot 1993 for details). Independently of the details of the model, the probability density peaks at  $z_f \sim 1$ .

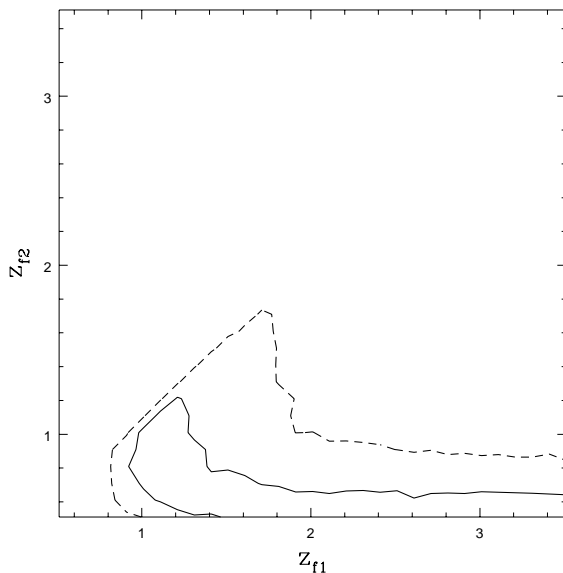


Figure 5. Model with two simple populations of stars. The older is formed at  $z_{f1}$ , the younger, with a tenth of the mass, is formed at  $z_{f2}$ . Contour levels of the *a posteriori* probability are shown as solid (68 %) and dashed (95%) lines.